Basic

European Journal of Immunology

Adaptive immunity

Research Article

Curtailed T-cell activation curbs effector differentiation and generates CD8$^+$ T cells with a naturally-occurring memory stem cell phenotype

Veronica Zanon[1], Karolina Pilipow[1], Eloise Scamardella[1], Federica De Paoli[1], Gabriele De Simone[1], David A. Price[2], Amaia Martinez Usatorre[3], Pedro Romero[3], Domenico Mavilio[4,5], Alessandra Roberto[1] and Enrico Lugli[1,6]

[1] Laboratory of Translational Immunology, Humanitas Clinical and Research Center, Rozzano, Milan, Italy
[2] Institution of Infection and Immunity, Cardiff University School of Medicine, Cardiff, Wales, UK
[3] Translational Tumor Immunology Group, Ludwig Center for Cancer Research, Epalinges, Switzerland
[4] Unit of Clinical and Experimental Immunology, Humanitas Clinical and Research Center, Rozzano, Milan, Italy
[5] Department of Medical Biotechnologies and Translational Medicine (BioMeTra), University of Milan, Italy, Milan
[6] Humanitas Flow Cytometry Core, Humanitas Clinical and Research Center, Rozzano, Milan, Italy

Human T memory stem (T_{SCM}) cells with superior persistence capacity and effector functions are emerging as important players in the maintenance of long-lived T-cell memory and are thus considered an attractive population to be used in adoptive transfer-based immunotherapy of cancer. However, the molecular signals regulating their generation remain poorly defined. Here we show that curtailed T-cell receptor stimulation curbs human effector CD8$^+$ T-cell differentiation and allows the generation of CD45RO$^-$CD45RA$^+$CCR7$^+$CD27$^+$CD95$^+$ -phenotype cells from highly purified naïve T-cell precursors, resembling naturally-occurring human T_{SCM}. These cells proliferate extensively in vitro and in vivo, express low amounts of effector-associated genes and transcription factors and undergo considerable self-renewal in response to IL-15 while retaining effector differentiation potential. Such a phenotype is associated with a lower number of mitochondria compared to highly-activated effector T cells committed to terminal differentiation. These results shed light on the molecular signals that are required to generate long-lived memory T cells with potential application in adoptive cell transfer immunotherapy.

Keywords: Adoptive cell transfer · CD8$^+$ · Effector T cells · T-cell activation · T memory stem cells

Additional supporting information may be found in the online version of this article at the publisher's web-site

Introduction

Specific antigen recognition by the T-cell receptor initiates a program of clonal expansion and effector differentiation in naïve T (T_N) cells that allows the migration to peripheral tissue and removal of infected targets [1]. Following resolution of the infection, most of these effector T cells die, leaving a population of long-lived memory T cells that is capable of more rapid and enhanced response following a second encounter with the pathogen [1]. The memory T-cell compartment is highly heterogeneous [2], comprising subsets that are different at the gene expression, metabolic and epigenetic level [3]. Current models suggest that circulating memory T cells are maintained in a stem cell-like fashion, were less differentiated cells self renew while generating more differentiated progeny with enhanced killing capacity [4]. Such heterogeneity

Correspondence: Dr. Enrico Lugli
e-mail: enrico.lugli@humanitasresearch.it

is important for anti-tumor immunity, specifically in the context of adoptive cell transfer (ACT) immunotherapy [4]. Indeed, preclinical and clinical evidence demonstrated that T cells committed to terminal differentiation, such as effector memory (T_{EM}) or terminal effector T (T_{TE}) cells, are poorly effective in mediating tumor regression following ACT [5]. Rather, less differentiated T stem cell memory (T_{SCM}) and central memory T (T_{CM}) are more potent in this regard because capable to persist in the long-term [6–10].

The clinical use of these memory T cells has been hampered by their limited number in the peripheral blood and at the tumor site, thus methods have been proposed to expand the pool of existing T_{SCM} by homeostatic cytokines [11] or to arrest differentiation of the more abundant T_N precursors [8, 12–15]. T_N activation with αCD3/2/28 antibody-conjugated beads in the presence of the glycogen synthase kinase-3β (GSK-3β) inhibitor TWS119 blocked differentiation and generated $CD45RO^-CCR7^+CD95^+$ T_{SCM}-like cells with improved anti-tumor immunity [8]. However, TWS119 decreases cell viability [12] and inhibits T-cell proliferation [8, 13]. The addition of IL-7 and IL-21 to the stimulation cocktail expanded the initial cell number by ~6-fold and allowed to generate naturally-occurring T_{SCM} [14]. Similarly, IL-7 and IL-15 in combination with strong αCD3/28 stimulation (3 beads: 1 cell) induced T_{SCM}-like cells with a hybrid $CD45RO^+CD45RA^+$ phenotype that is rarely found in vivo [13]. Nevertheless, they were endowed with superior persistence capacity in xenogeneic models compared to T_{CM} and T_{EM}. In summary, the use of specific combinations of cytokines or inhibition of specific signaling pathways have been demonstrated to arrest T-cell differentiation, but the specific role of potency of TCR stimulation as regards to the generation of T_{SCM} cells remains ill-defined.

Here we show that decreased TCR stimulation, achieved either by using a low αCD3/28 bead:cell ratio or by limiting the stimulation through the CD3 receptor, in the presence of IL-7 and IL-15 favors the generation of T_{SCM} cells with a naturally-occurring $CD45RA^+CD45RO^-$ phenotype. Such differentiation is associated with decreased T-cell activation and expression of effector-associated transcripts and transcription factors.

Results

Curtailed T-cell receptor stimulation in combination with IL-7 and IL-15 generates T_{SCM} cells

We first evaluated the effect of different cytokines, either alone or in combination, and potency of TCR stimulation on the differentiation of purified human peripheral blood T_N cells (Supporting Information Fig. 1) as assessed by surface expression of CD45RO and CCR7. We decided to use a low (i.e., 1:2) bead:cell ratio, as a previous report using a 3:1 ratio was associated with the acquisition of CD45RO by differentiating T_N [13]. Overall, IL-7 and IL-15 combined with αCD3/28 was the best combination to maintain a $CD45RO^-CCR7^+$ phenotype (Fig. 1A) and to generate bona fide $CD45RO^-CD45RA^+CCR7^+CD27^+CD95^+$ T_{SCM}-like cells (Fig. 1B; hereafter referred to as iT_{SCM}). By contrast, T-cell activation with αCD3/2/28 in the presence of IL-7/IL-15 or IL-2 preferentially generated $CD45RO^+CCR7^+$ T_{CM}-like cells (Fig. 1A and C). The addition of IL-18 to IL-2 stimulation had limited effect on T-cell phenotypes compared to IL-2 alone, while the addition of IL-12 generated bona fide $CD45RO^+CD45RA^-CCR7^-CD27^{int}CD95^+$ T effectors (iT_{Eff}) (Fig. 1A–B). Besides differential expression of known T-cell differentiation markers, iT_{SCM} also displayed lower CD38 and HLA-DR (indicative of activation) and Ki-67 (proliferation) compared to iT_{Eff} (Fig. 1B) and had lower forward scatter (FSC, indicative of cell size). A summary of the T-cell differentiation phenotypes (defined in Materials and methods) induced by selected culture conditions is shown in Fig. 1C. Overall, more potent stimulation due to triggering of CD2 significantly increased the frequency of non-viable cells at the end of the culture period, irrespectively of the cytokine cocktail (Fig. 1D). In iT_{Eff} condition, this was compensated by increased proliferation (Fig. 1E). Despite the lower proliferation and activation compared to iT_{Eff} in vitro, iT_{SCM} cells expanded robustly over time in vivo following adoptive transfer into NSG mice (Fig. 1F) and infiltrated multiple organs, including the spleen, the liver and, at a lesser extent, the lung (Fig. 1G).

Polyclonal and antigen-specific T_{SCM} cells are early-differentiated T cells

The capability to produce effector cytokines following TCR stimulation is shaped by the degree of memory differentiation, where less differentiated T cells mainly produce IL-2 and TNF while more differentiated ones mainly produce IFN-γ [16]. We therefore reasoned that iT_{SCM} and iT_{Eff} had different patterns of cytokine production. To test this, day 12 iT_{SCM} were re-stimulated with PMA/ionomycin (P/I) for 3 h. Figures 2A and D show that iT_{SCM} mainly produced TNF and IL-2, either in combination or alone, but little IFN-γ, while iT_{Eff} were mostly characterized by cells producing the 3 cytokines together. To confirm that the same pattern of functionality could be observed at the antigen-specific level, we took advantage of an accelerated DC maturation protocol [17] and of the elevated frequency of Mart-1-specific $CD8^+$ T cells to generate antigen-specific T_{SCM} cells from T_N precursors. To this end, we stimulated PBMCs from HLA-A*02^+ donors with the native, 10-mer Mart-1 peptide EAAGIGILTV, or its heteroclitic variant ELAGIGILTV, that is capable to bind cognate TCRs with higher avidity (hereafter named EAA and ELA, respectively). Both peptides primed a $CD8^+$ proliferative response, as assessed by CFSE dilution and tetramer staining (Fig. 2B), although ELA generated a higher frequency of antigen-specific T cells as well as a higher total count of antigen-specific T_{SCM} cells compared to EAA (Fig. 2C). Subsequent ELA-peptide restimulation 7 days post initial priming induced antigen-specific cytokine production in both $CD8^+$ populations (Supporting Information Fig. 3). Among these, $CD45RO^-CCR7^+CD95^+$ T_{SCM}-phenotype cells had a similar pattern of IFN-γ, IL-2, and TNF expression, irrespectively of the

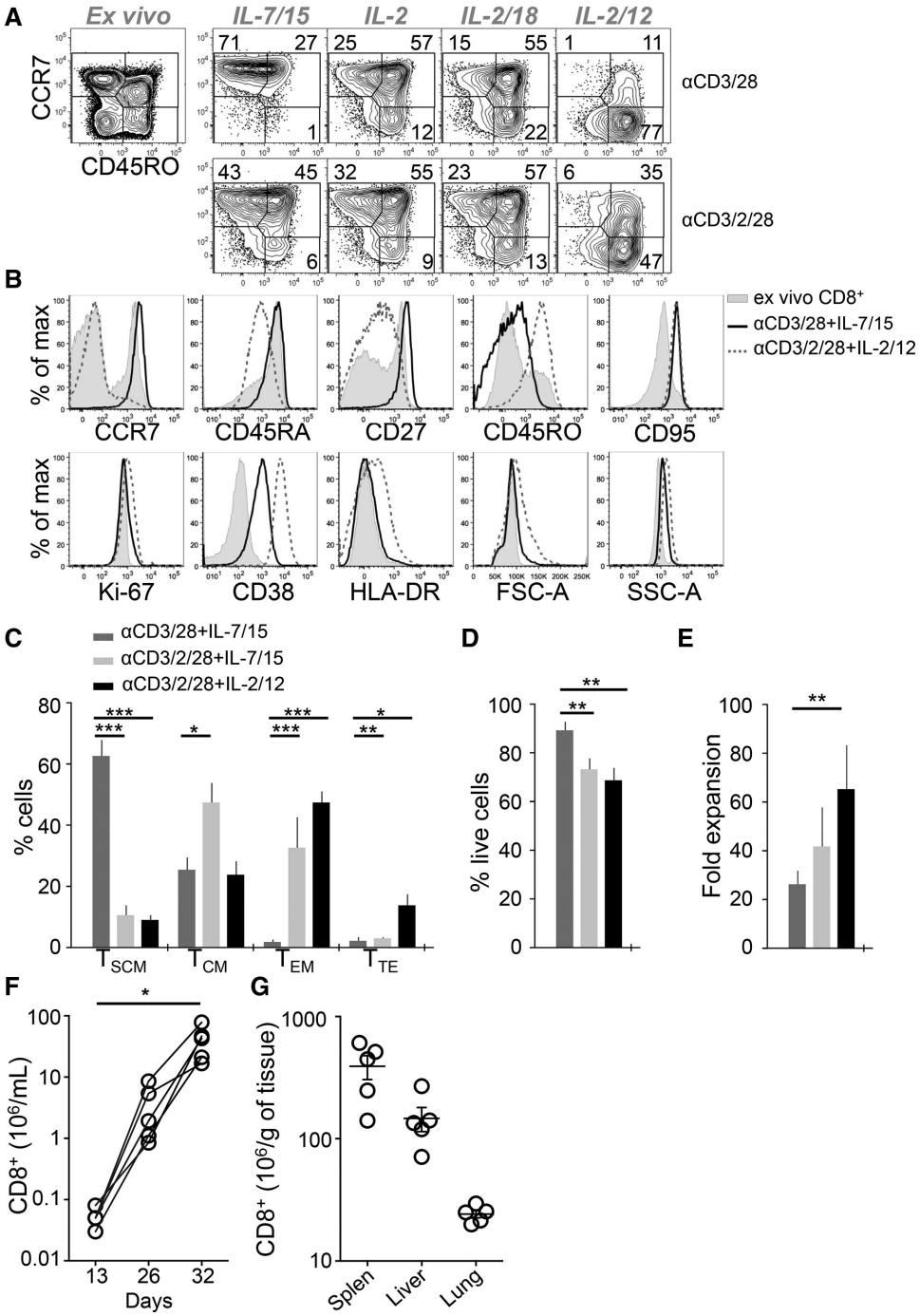

Figure 1. Generation of iT_{SCM} cells. (A) Representative expression of CD45RO and CCR7 in ex vivo PBMCs and in sorted $CD8^+$ T_N cells as evaluated by flow cytometry following culture with different cytokine cocktails and T-cell receptor dependent stimulation for 11 days. Similar data were obtained from a second donor. (B) Sorted $CD8^+$ T_N cells were cultured in αCD3/28+IL-7/15 or αCD3/2/28+IL-2/12 for 11 days and the expression of naïve and memory-associated markers in the two conditions (black line histogram and dashed line histogram, respectively; $n = 4$ for all parameters, except $n = 2$ for Ki-67, CD38, and HLA-DR) was evaluated as in (A), by flow cytometry. Total $CD8^+$ T cells from a healthy donor were used as control staining (ex vivo $CD8^+$; filled gray histogram). (C) The proportion of $CD8^+$ T cells with the T_{SCM}, T_{CM}, T_{EM}, and T_{TE} phenotypes (gated as in Supporting Information Fig. 1) after culture in the indicated conditions (αCD3/28+IL-7/15: $n = 22$; αCD3/2/28+IL-7/15: $n = 9$; αCD3/2/28+IL-2/12: $n = 12$) for 11 days was determined by flow cytometry and shown as mean ± SEM. (D) Mean + SEM of the percentage of viable cells and (E) fold expansion in cell number, compared to baseline, of sorted $CD8^+$ T_N cells cultured as in C. (F, G) Human $CD8^+$ T_N cells cultured in αCD3/28+IL-7/15 were transferred into NSG mice and at the indicated days after transfer, the (F) absolute numbers of $CD8^+$ T cells in the circulation, and (G) those cells infiltrating different organs at necropsy 32 days post transfer were evaluated by flow cytometry (see Supporting Information Fig. 2 for the gating strategy). Data shown as mean±SEM of 5 replicate mice, one single experiment. $^*p < 0.05$, $^{**}p < 0.01$, and $^{***}p < 0.001$, Wilcoxon test.

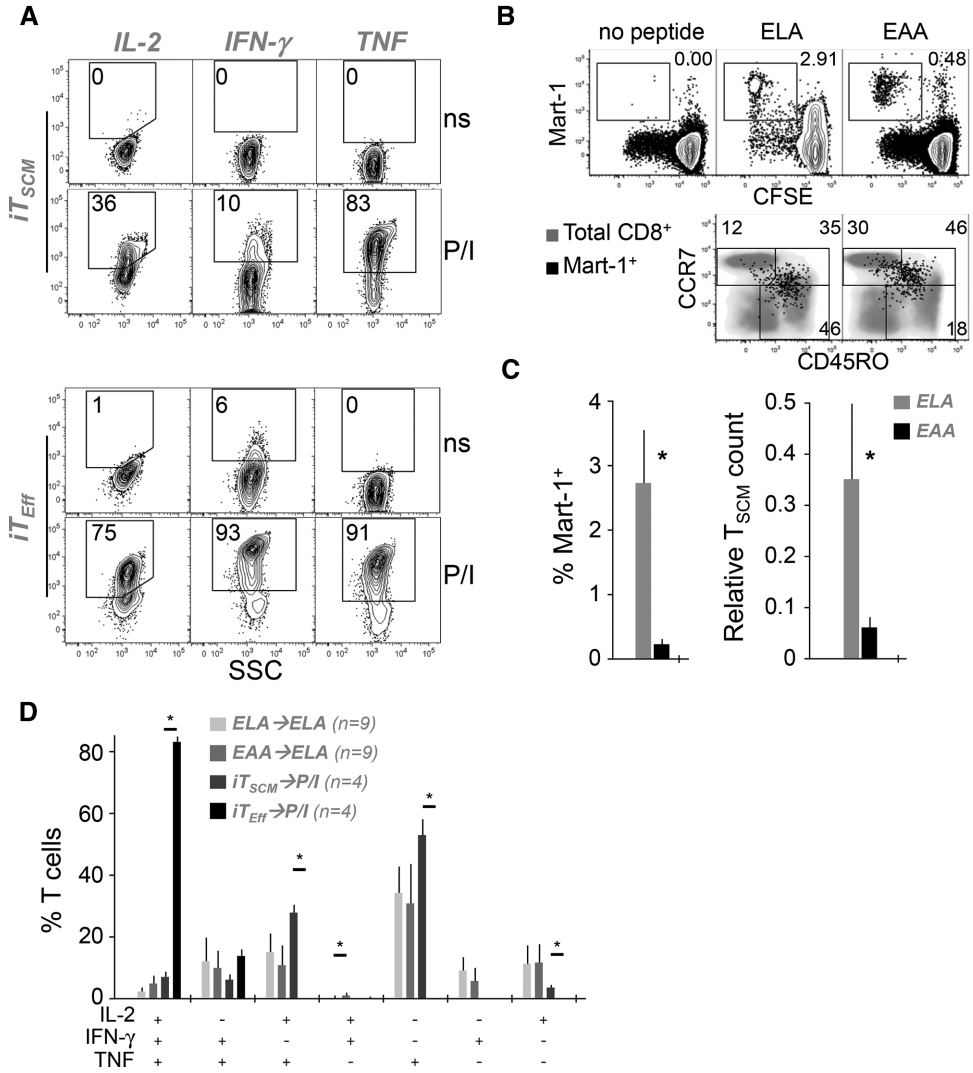

Figure 2. Polyclonal and antigen-specific T_{SCM} cells are early-differentiated T cells. (A) CD8+ T_N cells were activated as in Fig. 1C to generate iT_{SCM} and iT_{Eff}. Representative IL-2, IFN-γ and TNF expression in iT_{SCM} cells and iT_{Eff} cells following PMA/ionomycin (P/I) stimulation was evaluated by intracellular flow cytometry staining; ns: nonstimulated. (B) HLA-A*02$^+$ PBMCs from healthy donors were stimulated with FLT-3, IL-1β, PGE-2 and TNF (DC maturation/activation mix, day 0) and Mart1 peptide and IL-7 and IL-15 (day 1). Representative CFSE dilution and frequency of Mart-1-specific CD8$^+$ T cells (top) and CD45RO and CCR7 expression in Mart-1$^+$ cells (black) superimposed to total CD8$^+$ T cells from the same culture (bottom) as assessed by flow cytometry. Data shown are representative of nine other measurements from four independent experiments (C) The frequency of Mart-1$^+$ among CD8$^+$ cells (left; ELA: $n = 6$; EAA: $n = 9$) and the relative T_{SCM} count (right; ELA: $n = 6$; EAA: $n = 5$) following peptide stimulation is shown as mean + SEM. Relative T_{SCM} count was calculated only when the total number of cells within the Mart-1$^+$ fraction was >15. (D) The production of IL-2, IFN-γ and TNF following PMA/ionomycin (P/I) stimulation of cells obtained as in (A) or following ELA Mart-1 peptide stimulation of cells obtained as in (B) was measured by flow cytometry. Data shown as mean + SEM; 5 independent experiments. The number of independent donors tested is indicated in the figure. The legend refers to the initial stimulation at day 0 and to the restimulation at day 7 (either ELA peptide or P/I). In all flow cytometry plots, values indicate percentage of cells within the gate. $^*p < 0.05$ versus iT_{SCM}, Wilcoxon test.

original peptide used for their generation, that was mostly comparable to that of iT_{SCM} generated by αCD3/28 beads and restimulated with P/I (Fig. 2D).

iT_{SCM} cells undergo limited activation and effector differentiation

To gain more mechanistic insights into the differentiation of purified T_N cells toward the iT_{SCM} phenotype, we quantified the level of molecules, either at the protein or mRNA level, that are responsible for effector differentiation. Specifically, transcription factors T-bet and Eomes control effector T-cell function [18, 19] and increase progressively with human peripheral differentiation [8], while IRF4 [20], IRF8 [21], and miR-155 [22] are mostly regulated by the potency of TCR activation. Accordingly, T-bet and Eomes increased progressively with the duration of the culture period (Fig. 3A), while IRF4, IRF8, and miR-155 were mostly detected during the first week of culture, then their expression waned (Fig. 3B). Overall, these molecules were generally

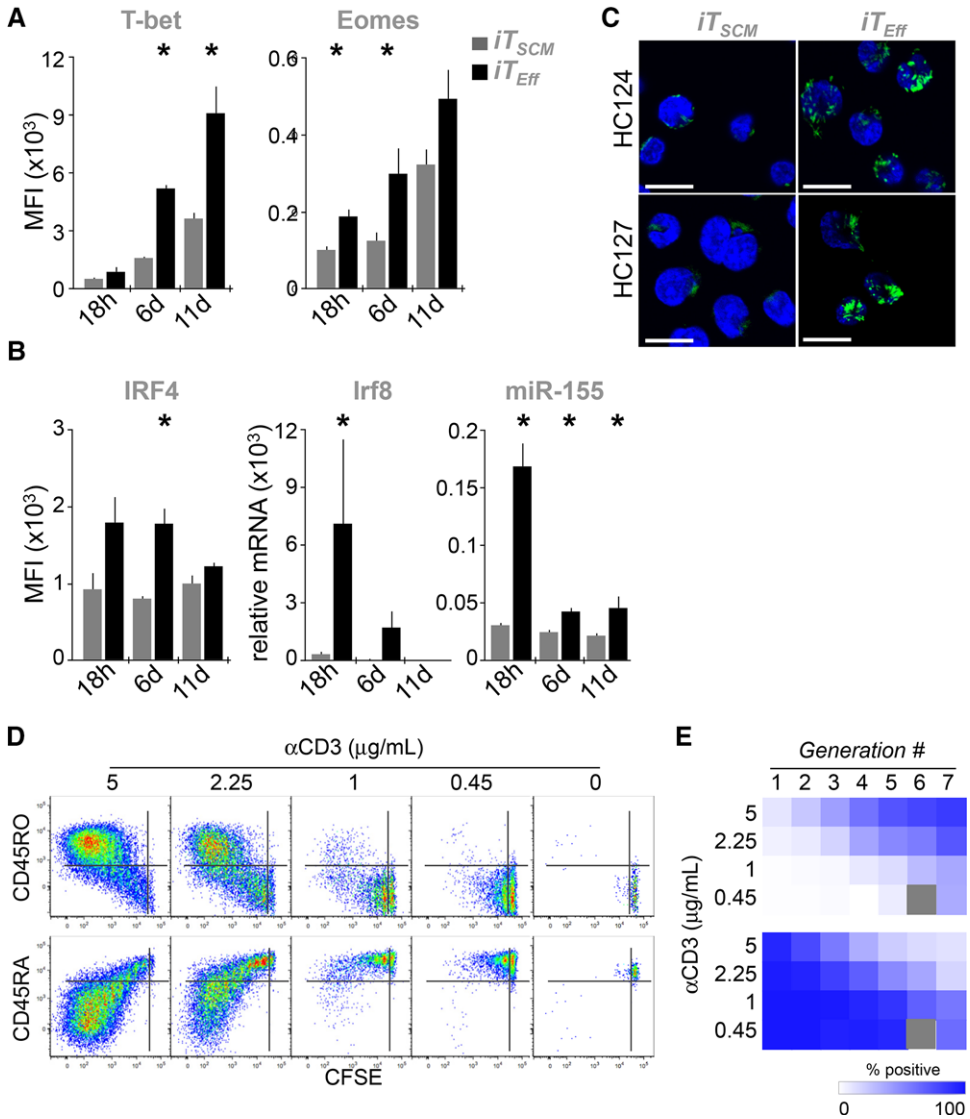

Figure 3. iT_{SCM} cells undergo limited activation and effector differentiation. (A, B) $CD8^+$ T_N cells were stimulated with αCD3/28+IL-7/15 (iT_{SCM} condition) or αCD3/2/28+IL-2/12 (iT_{Eff} condition) and evaluated for the expression of multiple effector molecules either by flow cytometry (T-bet, Eomes, IRF4; expressed as median fluorescence intensity or MFI; $n = 3$) or by RT-qPCR (Irf8, miR-155; $n = 4$). h, hours; d, days. Data shown as mean + SEM of the indicated numbers of samples from a single experiment. $^*p<0.05$ versus iT_{SCM}, Wilcoxon test. (C) Confocal microscopy analysis (100× magnification) of mitotracker green (staining mitochondria; in green) and DAPI (staining nuclei; in blue) in iT_{SCM} cells and iT_{Eff} cells generated from $CD8^+$ T_N cells as in A. Figure shows cells from two different individuals. Similar data were obtained from two more individuals. Scale bars, 10 μM. (D) Representative flow cytometry analysis of CD45RO (top) and CD45RA (bottom) in CFSE-diluting $CD8^+$ T_N cells following stimulation with different concentrations of plate-bound αCD3 and 5 μM soluble αCD28. (E) Heat map of data as in (D) according to CFSE generation ($n = 1$–4, depending on cell count/cycle; gray box: data not available due to the low cell count).

overexpressed in iT_{Eff} vs. iT_{SCM} throughout the stimulation period, thus recapitulating the differential activation status observed in Fig. 1B and indicating limited activation and effector differentiation of iT_{SCM} cells. It has also been proposed that subsets of T cells at different stages of differentiation harbour different numbers of mitochondria, where the mitochondrial content increases with progressive differentiation of T cells isolated ex vivo ($T_N<T_{CM}<T_{EM}$) [23]. Single cell analysis by confocal microscopy revealed that iT_{SCM} harbored fewer mitochondria and appeared to have little cytoplasm compared to iT_{Eff} (Fig. 3C), thus corroborating the lower FSC levels observed in Fig. 1B.

Despite using a low bead:cell ratio to generate T_{SCM} with the naturally-occurring $CD45RO^-$ $CD45RA^+$ phenotype, it is difficult to evaluate the specific contribution of CD3 and CD28 molecules in this regard. To this aim, we stimulated T_N cells in T_{SCM}-promoting conditions (i.e., with IL-7 and IL-15) and in the presence of titrated amounts of plate-bound αCD3 and soluble αCD28, then assessed CD45RA and CD45RO expression (Fig. 3D; Supporting Information Fig. 4). Phenotypic dynamics depend on the level of proliferation [24]. As different strenghts of TCR stimulation result in differential proliferation, analysis of specific markers was performed according to the level of CFSE dilution (i.e., generations)

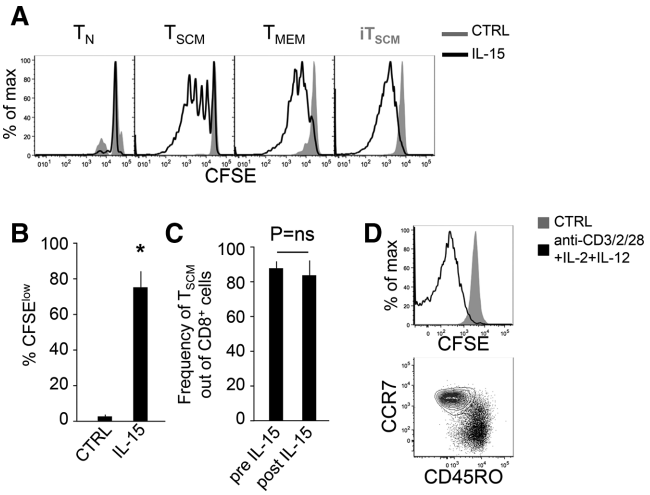

Figure 4. Self-renewing and multipotent capacity of iT_{SCM} cells. (A) Ex vivo sorted T_N, T_{SCM}, and total memory T (T_{MEM}; defined as $CD45RO^+$; Supporting Information Fig. 1) $CD8^+$ T cells as well as iT_{SCM} (generated as in Fig. 1C) were incubated with IL-15 for 12 days (black line histogram). CFSE dye dilution was measured by flow cytometry. Filled gray histogram indicates unstimulated control. (B) The percentage of CFSE-diluting cells in (A) is shown as mean±SEM of $n = 4$ samples from two independent experiments ($n = 2$ each). $^*p<0.05$ versus CTRL, Wilcoxon test. (C) The frequency of T_{SCM}-phenotype cells (defined as in Supporting Information Fig. 1) out of total $CD8^+$ T cells after stimulation of T_N cells for 6 days in iT_{SCM} polarizing conditions (pre IL-15) or after stimulation of the same iT_{SCM} with IL-15 for 12 days (post IL-15) was measured by flow cytometry. Data are shown as mean±SEM of $n = 4$ samples as in B. (D) CFSE dilution (top) and CD45RO and CCR7 expression following αCD3/2/28 + IL-2 and IL-12 stimulation (bottom) of iT_{SCM} cells generated as in Fig. 1C was measured by flow cytometry. Data shown are representative of measurements made for three samples from two independent experiments.

when >50 cells were available in each gate. Changing the concentration of αCD28 had no impact on T-cell phenotypes (not shown), while decreasing αCD3 resulted in the progressive shift of proliferating cells toward a $CD45RO^-$ $CD45RA^+$ phenotype (Fig. 3D–E, Supporting Information Fig. 4). These cells also maintained the expression of CCR7 and CD27 and de novo expressed CD95 (Supporting Information Fig. 4), confirming that curtailed TCR stimulation favors the generation of T_{SCM} cells.

Self-renewing and multipotent capacity of iT_{SCM} cells

Naturally-occurring T_{SCM} are known to preferentially self-renew in vitro and in vivo compared to T_{CM} and T_{EM}, while simultaneously capable to generate more differentiated progeny [8, 9, 25]. To assess both these aspects respectively, iT_{SCM} were collected 7 days following stimulation, stained with CFSE and induced to proliferate in response to the homeostatic cytokine IL-15 or to αCD3/2/28 beads +IL-2 and IL-12 (iT_{Eff}-polarizing condition). According to their memory properties, iT_{SCM} proliferated in response to IL-15 similarly to ex vivo T_{SCM} and bulk memory T cells (T_{MEM}; sorted as $CD45RO^+$), while ex vivo T_N were non-proliferating (Fig. 4A), as previously described [8, 9, 11]. A summary of CFSE dilution from 4 donors is shown in Fig. 4B. Similar proliferation could be observed following iT_{Eff}-polarizing condition. While T cells in IL-15 largely maintained their original phenotype (Fig. 4C), those in iT_{Eff}-polarizing condition differentiated to $CD45RO^+CCR7^+$ T_{CM} and $CD45RO^+CCR7^-$ T_{EM} cells (Fig. 4D), thus indicating self-renewal capacity and multipotency, respectively.

Discussion

We show that curtailed T-cell receptor stimulation favors the generation of early-differentiated $CD45RO^-$ $CD45RA^+$ T_{SCM} cells from naïve precursors, and that this is associated with restrained T-cell activation and upregulation of transcriptional regulators that are otherwise responsible for effector differentiation. Similar phenotypes could be obtained by using Dynabeads from Thermo Fisher (data not shown), that are currently being used to expand T cells in ACT clinical trials. Such molecular dynamics were evident since the very first hours following stimulation in vitro. These data are important as increasing evidence in preclinical models and in humans indicate that T cells at earlier stages of differentiation, such as T_{SCM} and T_{CM} cells are better suited to persist long-term in vivo following adoptive transfer and are endowed with more potent activity, such as that directed toward tumors [26].

By separately testing molecules involved in T-cell activation and by titrating the amount of signal delivered to T cells, we found a role for CD3, but not for CD28 in defining the acquisition of the $CD45RO^-$ $CD45RA^+$ T_{SCM} phenotype. These iT_{SCM} were both self-renewing and multipotent and had features of early-differentiated T cells in terms of cytokine production profile in response to polyclonal and antigen specific stimulation. Indeed, in vitro priming of T_N cells with the native self/tumor antigen Mart-1 EAA, and its heteroclitic variant ELA, results in the generation of a subset of T_{SCM} cells with functional capacity that is similar to iT_{SCM} generated by polyclonal stimulation. Despite priming less T_N precursors due to its decreased binding strength to the TCR, which results in a lower total number of Mart-1-specific $CD8^+$ T cells (Fig. 2B), EAA selects those TCRs with the highest avidity that is in turn associated with more pronounced anti-tumor activity [27]. It has been therefore speculated that EAA is preferable to ELA in vaccine regimens. ELA/EAA peptide vaccination in combination with CpG and Montanide in melanoma patients resulted in the early (<3 months) generation of Mart-1-specific T_{SCM} cells that were capable to persist in the long term [27]. However, antigen-specific T_{SCM} generation was shown to occur much earlier, such as following infection with simian immunodeficiency virus (SIV) in rhesus macaques, where SIV-specific T_{SCM} cells developed as early as 7 days after infection, expanded clonally and coincidentally with the differentiation of bona fide T_{Eff}. Interestingly, a much lower proportion of TSCM displayed expression of HLA-DR and Ki-67 activation markers compared to T_{Eff}, while preferentially expressing transcripts involved in T-cell survival and persistence such as *MCL1*, *BCL2,* and *LEF1* [9]. Overall, this could reflect limited TCR stimulation occurring in vivo.

iT_{SCM} differentiation also resulted in a lower mitochondrial content. In line with our results, Akbar and colleagues analyzed

human $CD8^+$ T-cell subsets sorted ex vivo by transmission microscopy and revealed that mitochondrial content increases progressively in human T_{CM} and T_{EM} compared to T_N [23]. Differently Van der Windt et al., reported a higher mitochondrial content in cells kept in IL-15 compared to those kept in IL-2 [28]. Differences in protocols used to generate memory precursors could explain these contrasting results. In fact, Van der Windt et al. generated memory T cells by initially activating T_N in the presence of IL-2 for 3 days, followed by a switch in IL-15 for 2 additional days, thus leading to hypothesize that IL-2 stimulation, although transient, has long term effect on T-cell metabolism. While initial exposure to IL-2 might better mimic the in vivo condition during effector differentiation, IL-2 stimulation in vitro should be avoided when generating T cells for ACT, because inducing more committed differentiation (Fig. 1A) [29], and loss of anti-tumor capacity [14].

Inhibition of effector differentiation of T_N precursors has been achieved in multiple ways, such as pharmacological intervention, cytokine cocktails and genetic manipulation [26]. More recently, inhibition of bromodomain and extra-terminal motif (BET) proteins has been shown to limit BATF expression and favor the generation of T_{SCM} from human T_N [30]. The same group reported similar findings when stimulating bulk T cells with cell-based artificial antigen-presenting cells expressing ligands for CD3 and CD28 only transiently [31]. Of note, BATF is part of a multiprotein DNA-binding complex comprising Jun and IRF4 or IRF8 and is involved in the generation of effector T cells [32]. Our observations suggest that low but detectable levels of IRF4 and IRF8 are necessary for initial T-cell activation induced by the TCR but are dispensable for the generation of iT_{SCM}. We propose that limiting TCR stimulation during priming, and so the expression of transcriptional regulators of effector differentiation can be exploited as an additional strategy to generate iT_{SCM} for ACT immunotherapy.

Materials and methods

Mice

All animal experiments were conducted upon the approval of the Humanitas IACUC and the Italian Ministry of Health (protocol 256/2015-PR). NOD.Cg-*Prkdc*^{scid} *Il2rg*^{tm1Wjl}/SzJ (NSG) mice (Jackson Laboratories), bred in SPF conditions, were used for adoptive transfer experiments. Briefly, 1–2 $\times$ 10^6 $CD8^+$ T cells, expanded in vitro with αCD3/28-conjugated beads (T-cell activation/expansion kit, Miltenyi; 1 bead:2 cells), were co-transferred by retrorbital injection with 8 $\times$ 10^6 PBMCs depleted of $CD8^+$ T cells. For mononuclear cell isolation, tissues were minced and filtered through a 100 μM cell strainer.

Cells

All experiments were approved by the Humanitas Research Hospital IRB. Peripheral blood mononuclear cells (PBMCs) were isolated from buffy coats and frozen in liquid nitrogen according to standard procedures.

Flow cytometry and cell sorting

Fluorochrome-conjugated monoclonal antibodies were purchased from BD Biosciences, Biolegend and eBioscience (see Supporting Information Table 1 for details), and titrated to determine optimal concentration. Either fresh or frozen cells were used. Frozen cells were thawed and stained for flow cytometry as described [11]. HLA-A*0201/MART-126-35 ELAGIGILTV tetramer staining (conjugated to streptavidin-BV421) was performed at 37°C for 20 min. Intracellular transcription factors were detected following fixation of cells with the FoxP3/transcription factor staining buffer set (eBioscience). T-cell subsets were defined as follows: T_N, $CD45RO^-CD45RA^+CCR7^+CD27^+CD95^-$; T_{SCM}, $CD45RO^-CD45RA^+CCR7^+CD27^+CD95^+$; T_{CM}, $CD45RO^+CCR7^+$; T_{EM}, $CD45RO^+CCR7^-$; T_{TE}, $CD45RO^-CCR7^+$; bulk memory T (T_{MEM}) cells: $CD45RO^+$ [11]. T_N were FACS-sorted as depicted in Supporting Information Fig. 1. Samples were acquired on a Fortessa flow cytometer or separated via a FACS Aria III cell sorter (all from BD Biosciences). Flow cytometry data were compensated with FlowJo (FlowJo LLC) by using single-stained controls prepared with antibody-capture beads (BD Biosciences).

Cell culture

PBMC or sorted T cells (0.25 $\times$ 10^6 cells/mL) were cultured in complete RPMI medium (10% FBS, 1% penicillin/streptomycin, 2 mM L-glutamine), and stimulated with αCD3/2/28 antibody-coated beads. When preparing beads bound to αCD3/28 only, the amount of αCD2 in the mix was replaced by PBS (without calcium and magnesium, referred to as $PBS^{-/-}$). Alternatively, cells were stimulated with plate-bound αCD3 (clone OKT3) plus soluble CD28 (clone CD28.2) in 96 flat-bottomed wells for 9 days. Human cytokines (Peprotech) were pre-titrated, then used at 10 ng/mL unless specified. Cell proliferation was determined by the analysis of CFSE (5 μM; Life Technologies) dilution [11]. Cells were subsequently stimulated with IL-15 (Peprotech) for 12 days at 50 ng/mL, or left in 1 ng/mL IL-15 (non-proliferating control). Cell number was determined by Trypan blue dye exclusion.

To induce cytokine production by PMA/ionomicin stimulation and to measure intracellular cytokine production, cells were treated as described [33].

Antigen-specific T cells were grown by using an accelerated DC maturation protocol, as described [17]. Briefly, 3.5 $\times$ 10^6 CFSE-stained PBMCs from HLA-A*02^+ donors were plated in 48-well plates in AIM-V medium (Life Technologies) additioned with FLT-3 (50 ng/mL; DC maturation) on day 0 and with IL-1β, PGE-2, TNF (DC activation mix) and the Melan-A/Mart1 petide variants ELAGIGLTV or EAAGIGILTV (2 μg/mL; peptide chemistry facility, University of Lausanne) on day 1. IL-7 and IL-15 (both

at 10 ng/mL) were included in each well on day 1. Cells were collected at day 7 for FACS analysis, otherwise restimulated with 2 μg/mL ELAGIGLTV for 18 h in the presence of GolgiPlug (BD Biosciences), according to manufacturer's instructions.

Real-time PCR (qPCR)

Total RNA, purified with RNeasy Micro Kit (Qiagen), was retrotranscribed using High-capacity cDNA Reverse Transcription Kit (Applied Biosystems) and analyzed by qPCR with hydrolysis probes: *IRF8* (Hs00175238_m1) and *18S* (Hs99999901_s1) as reference gene (Applied Biosystems) using the ABI 7900HT Sequence Detection System (Applied Biosystems). For Micro-RNA (miR) expression analysis, RNA was isolated with mirVana kit (Ambion). Mature miR-155 and RNU44 small nucleolar RNA were reverse transcribed with specific primers provided by Applied Biosystems and TaqMan RT MicroRNA Kit (Applied Biosystems). qPCR was performed with miR-155 and RNU44 specific TaqMan primers (Applied Biosystems) and Universal PCR Master Mix, No AmpErase® UNG (Roche) in MicroAmp® Fast Optical 96-Well Reaction Plate (Applied Biosystems) on a 7500 Fast Real-Time PCR System (Applied Biosystems). Expression levels were normalized (ΔCt) to RNU44 or 18S endogenous controls and expression fold change relative to $CD8^+$ T_N cells were calculated using $2^{-(\Delta Ct\ sample - \Delta Ct\ naive)}$ formula.

Confocal microscopy

$CD8^+$ T cells were washed in $PBS^{-/-}$ and incubated with 1 mL of pre-warmed Mitotracker Green (25nM prepared in $PBS^{-/-}$) for 30 min at 37°C. To allow T-cell adhesion, slides were previously incubated for 30 min with 0.02% polylisin and coated for 3 h at 37°C with αCD3 (OKT3 clone, BD Biosciences; 10 μg/mL in $PBS^{-/-}$) and αCD28 (CD28.2 clone, BD Biosciences; μg/mL in $PBS^{-/-}$) followed by 3 washes in $PBS^{-/-}$. T cells (0.15×10^6) were then layered on slides and incubated for 15 min at 37°C. After incubation, cells were fixed with 4% PFA for 10 min, washed twice with 2% BSA in $PBS^{+/+}$ and once with 2% BSA, 0.05% tween in $PBS^{+/+}$. To identify nuclei, cells were counterstained with DAPI (Invitrogen) by incubating for 10' at RT. Slides were acquired with an FV1000 confocal microscope (Olympus). Images were analyzed with ImageJ (NIH).

Statistical analysis

Analysis was performed using GraphPad PRISM (6.0b) and SPICE 5.22 software. Non-parametric paired or unpaired Wilcoxon rank test were used to compare two groups. *P* values are two-sided and were considered significant when ≤0.05.

Acknowledgements: The authors wish to thank Diego Morone (microscopy facility, Humanitas) for help with confocal analysis. This work was supported by grants from the European Research Council (ERC-StG-2014 PERSYST #640511), the Fondazione Cariplo (Grant Ricerca Biomedica 2012/0683), the Italian Ministry of Health (Bando Giovani Ricercatori GR-2011-02347324) and the European Union Marie Curie Career Integration Grant 322093 (all to E.L.). A.R. and E.S. are supported by fellowships from Fondazione Italiana per la Ricerca sul Cancro (FIRC). E.L. is an International Society for the Advancement of Cytometry (ISAC) Marylou Ingram scholar. D.A.P is a Wellcome Trust Senior Investigator.

Conflict of interest: The authors declare no financial or commercial conflict of interest.

References

1 **Kaech, S. M. and Ahmed, R.**, Memory CD8+ T cell differentiation: initial antigen encounter triggers a developmental program in naive cells. *Nat. Immunol.* 2001. **2**: 415–422.

2 **Mahnke, Y. D., Brodie, T. M., Sallusto, F., Roederer, M. and Lugli, E.**, The who's who of T-cell differentiation: human memory T-cell subsets. *Eur. J. Immunol.* 2013. **43**: 2797–2809.

3 **Man, K. and Kallies, A.**, Synchronizing transcriptional control of T cell metabolism and function. *Nat. Rev. Immunol.* 2015. **15**: 574–584.

4 **Gattinoni, L., Klebanoff, C. A. and Restifo, N. P.**, Paths to stemness: building the ultimate antitumour T cell. *Nat. Rev. Cancer* 2012. **12**: 671–684.

5 **Gattinoni, L., Klebanoff, C. A., Palmer, D. C., Wrzesinski, C., Kerstann, K., Yu, Z., Finkelstein, S. E. et al.**, Acquisition of full effector function in vitro paradoxically impairs the in vivo antitumor efficacy of adoptively transferred CD8+ T cells. *J. Clin. Invest.* 2005. **115**: 1616–1626.

6 **Zhang, Y., Joe, G., Hexner, E., Zhu, J. and Emerson, S. G.**, Host-reactive CD8+ memory stem cells in graft-versus-host disease. *Nat. Med.* 2005. **11**: 1299–1305.

7 **Berger, C., Jensen, M. C., Lansdorp, P. M., Gough, M., Elliott, C. and Riddell, S. R.**, Adoptive transfer of effector CD8+ T cells derived from central memory cells establishes persistent T cell memory in primates. *J. Clin. Invest.* 2008. **118**: 294–305.

8 **Gattinoni, L., Lugli, E., Ji, Y., Pos, Z., Paulos, C. M., Quigley, M. F., Almeida, J. R. et al.**, A human memory T cell subset with stem cell-like properties. *Nat. Med.* 2011. **17**: 1290–1297.

9 **Lugli, E., Dominguez, M. H., Gattinoni, L., Chattopadhyay, P. K., Bolton, D. L., Song, K., Klatt, N. R. et al.**, Superior T memory stem cell persistence supports long-lived T cell memory. *J. Clin. Invest.* 2013. **123**: 594–599.

10 **Graef, P., Buchholz, V. R., Stemberger, C., Flossdorf, M., Henkel, L., Schiemann, M., Drexler, I. et al.**, Serial transfer of single-cell-derived immunocompetence reveals stemness of CD8(+) central memory T cells. *Immunity* 2014. **41**: 116–126.

11 **Lugli, E., Gattinoni, L., Roberto, A., Mavilio, D., Price, D. A., Restifo, N. P. and Roederer, M.**, Identification, isolation and in vitro expansion

of human and nonhuman primate T stem cell memory cells. *Nat. Protoc.* 2013. **8**: 33–42.

12 **Forget, M. A., Huon, Y., Reuben, A., Grange, C., Liberman, M., Martin, J., Mes-Masson, A. M. et al.**, Stimulation of Wnt/ss-catenin pathway in human CD8+ T lymphocytes from blood and lung tumors leads to a shared young/memory phenotype. *PLoS One* 2012. **7**: e41074.

13 **Cieri, N., Camisa, B., Cocchiarella, F., Forcato, M., Oliveira, G., Provasi, E., Bondanza, A. et al.**, IL-7 and IL-15 instruct the generation of human memory stem T cells from naive precursors. *Blood* 2013. **121**: 573–584.

14 **Sabatino, M., Hu, J., Sommariva, M., Gautam, S., Fellowes, V., Hocker, J. D., Dougherty, S. et al.**, Generation of clinical-grade CD19-specific CAR-modified CD8+ memory stem cells for the treatment of human B-cell malignancies. *Blood* 2016. **128**: 519–528.

15 **Alvarez-Fernandez, C., Escriba-Garcia, L., Vidal, S., Sierra, J. and Briones, J.**, A short CD3/CD28 costimulation combined with IL-21 enhance the generation of human memory stem T cells for adoptive immunotherapy. *J. Transl. Med.* 2016. **14**: 214.

16 **Seder, R. A., Darrah, P. A. and Roederer, M.**, T-cell quality in memory and protection: implications for vaccine design. *Nat. Rev. Immunol.* 2008. **8**: 247–258.

17 **Briceno, O., Lissina, A., Wanke, K., Afonso, G., von Braun, A., Ragon, K., Miquel, T. et al.**, Reduced naive CD8(+) T-cell priming efficacy in elderly adults. *Aging Cell* 2016. **15**: 14–21.

18 **Pearce, E. L., Mullen, A. C., Martins, G. A., Krawczyk, C. M., Hutchins, A. S., Zediak, V. P., Banica, M. et al.**, Control of effector CD8+ T cell function by the transcription factor Eomesodermin. *Science* 2003. **302**: 1041–1043.

19 **Joshi, N. S., Cui, W., Chandele, A., Lee, H. K., Urso, D. R., Hagman, J., Gapin, L. et al.**, Inflammation directs memory precursor and short-lived effector CD8(+) T cell fates via the graded expression of T-bet transcription factor. *Immunity* 2007. **27**: 281–295.

20 **Man, K., Miasari, M., Shi, W., Xin, A., Henstridge, D. C., Preston, S., Pellegrini, M. et al.**, The transcription factor IRF4 is essential for TCR affinity-mediated metabolic programming and clonal expansion of T cells. *Nat. Immunol.* 2013. **14**: 1155–1165.

21 **Miyagawa, F., Zhang, H., Terunuma, A., Ozato, K., Tagaya, Y. and Katz, S. I.**, Interferon regulatory factor 8 integrates T-cell receptor and cytokine-signaling pathways and drives effector differentiation of CD8 T cells. *Proc. Natl. Acad. Sci. U S A* 2012. **109**: 12123–12128.

22 **Dudda, J. C., Salaun, B., Ji, Y., Palmer, D. C., Monnot, G. C., Merck, E., Boudousquie, C. et al.**, MicroRNA-155 is required for effector CD8+ T cell responses to virus infection and cancer. *Immunity* 2013. **38**: 742–753.

23 **Henson, S. M., Lanna, A., Riddell, N. E., Franzese, O., Macaulay, R., Griffiths, S. J., Puleston, D. J. et al.**, p38 signaling inhibits mTORC1-independent autophagy in senescent human CD8(+) T cells. *J. Clin. Invest.* 2014. **124**: 4004–4016.

24 **Brenchley, J. M., Douek, D. C., Ambrozak, D. R., Chatterji, M., Betts, M. R., Davis, L. S. and Koup, R. A.**, Expansion of activated human naive T-cells precedes effector function. *Clin. Exp. Immunol.* 2002. **130**: 432–440.

25 **Biasco, L., Scala, S., Basso Ricci, L., Dionisio, F., Baricordi, C., Calabria, A., Giannelli, S. et al.**, In vivo tracking of T cells in humans unveils decade-long survival and activity of genetically modified T memory stem cells. *Sci. Transl. Med.* 2015. **7**: 273ra13.

26 **Gattinoni, L., Speiser, D. E., Lichterfeld, M. and Bonini, C.**, T memory stem cells in health and disease. *Nat. Med.* 2017. **23**: 18–27.

27 **Gannon, P., Baumgaertner, P., Huber, A., Iancu, E. M., Cagnon, L., Abed-Maillard, S., Maby-El Hajjami, H. et al.**, Rapid and continued T cell differentiation into long-term effector and memory stem cells in vaccinated melanoma patients. *Clin. Cancer Res.* 2016. **23**: 3285–3296.

28 **van der Windt, G. J., Everts, B., Chang, C. H., Curtis, J. D., Freitas, T. C., Amiel, E., Pearce, E. J. et al.**, Mitochondrial respiratory capacity is a critical regulator of CD8+ T cell memory development. *Immunity* 2012. **36**: 68–78.

29 **Kalia, V., Sarkar, S., Subramaniam, S., Haining, W. N., Smith, K. A. and Ahmed, R.**, Prolonged interleukin-2Ralpha expression on virus-specific CD8+ T cells favors terminal-effector differentiation in vivo. *Immunity* 2010. **32**: 91–103.

30 **Kagoya, Y., Nakatsugawa, M., Yamashita, Y., Ochi, T., Guo, T., Anczurowski, M., Saso, K. et al.**, BET bromodomain inhibition enhances T cell persistence and function in adoptive immunotherapy models. *J. Clin. Invest.* 2016. **126**: 3479–3494.

31 **Kagoya, Y., Nakatsugawa, M., Ochi, T., Cen, Y., Guo, T., Anczurowski, M., Saso, K. et al.**, Transient stimulation expands superior antitumor T cells for adoptive therapy. *JCI Insight* 2017. **2**: e89580.

32 **Kurachi, M., Barnitz, R. A., Yosef, N., Odorizzi, P. M., DiIorio, M. A., Lemieux, M. E., Yates, K. et al.**, The transcription factor BATF operates as an essential differentiation checkpoint in early effector CD8+ T cells. *Nat. Immunol.* 2014. **15**: 373–83.

33 **Roberto, A., Castagna, L., Zanon, V., Bramanti, S., Crocchiolo, R., McLaren, J. E., Gandolfi, S. et al.**, Role of naive-derived T memory stem cells in T-cell reconstitution following allogeneic transplantation. *Blood* 2015. **125**: 2855–2864.

Abbreviations: **ACT**: adoptive cell transfer · **TCR**: T-cell receptor · T_N: naïve T cell · T_{SCM}: T stem cell memory · T_{CM}: central memory T cells · T_{EM}: effector memory T cells · T_{Eff}: effector T cell

Full correspondence: Dr. Enrico Lugli, Laboratory of Translational Immunology, Humanitas Clinical and Research Center, Via Alessandro Manzoni 113, Rozzano, Milan, Italy
Fax: +39-8224-5191
e-mail: enrico.lugli@humanitasresearch.it

Received: 20/9/2016
Revised: 22/5/2017
Accepted: 28/6/2017
Accepted article online: 3/7/2017